Engineering Notes

Satellite Attitude Stabilization Control with Actuator Faults

Senqiang Zhu,* Danwei Wang,† Qiang Shen,‡ and Eng Kee Poh§
Nanyang Technological University, Singapore 639798, Republic of Singapore

DOI: 10.2514/1.G001922

Nomenclature

$\boldsymbol{d}$	=	external disturbances
$\boldsymbol{E}$, $\hat{\boldsymbol{E}}$	=	actuator effectiveness and estimated effectiveness, respectively
$\boldsymbol{H}_{\text{rw}}$	=	reaction-wheel momentum
J, J_0, ΔJ	=	inertia matrix, nominal inertia matrix, and uncertainty in inertia matrix, respectively
J_{rw}	=	inertia of reaction wheel
L	=	positive definite gain matrix
M	=	distribution matrix
$[\boldsymbol{q}_v^T, q_0]^T$	=	unit quaternion
$\boldsymbol{u}$, $\boldsymbol{u}_c$	=	actual output torque and command torque of reaction wheels, respectively
$\bar{\boldsymbol{u}}$	=	bias fault
$\boldsymbol{\tau}$, $\boldsymbol{\tau}_c$	=	three-axis torque and three-axis torque command, respectively
$\boldsymbol{\Omega}$, $\hat{\boldsymbol{\Omega}}$	=	angular velocity and estimated angular velocity of reaction wheel, respectively
$\boldsymbol{\omega}$, $\hat{\boldsymbol{\omega}}$	=	angular velocity and estimated angular velocity of satellite, respectively

I. Introduction

IN RECENT years, more satellites were launched into space to perform various missions such as air navigation, communication, environmental monitoring, and military service. In most of these missions, attitude maneuver using actuators was required for satellites to achieve the desired attitude. However, an actuator fault or failure may cause significant performance degradation or even instability. The demand for satellite safety and reliability has spurred research on attitude fault-tolerant control (FTC) in the presence of actuator faults [1].

There are mainly two kinds of fault-tolerant control strategies: passive FTC and active FTC [2]. Passive FTC takes advantage of robust control techniques to ensure closed-loop system stability in the presence of actuator faults without requiring fault detection. In [3], an indirect robust adaptive FTC strategy was presented to deal with actuator failures for spacecraft attitude tracking. Using a backstepping technique, an adaptive FTC scheme was developed to achieve spacecraft attitude stabilization in [4], where actuator faults were estimated by three implicit estimation filters. Finite-time fault-tolerant attitude control was proposed in [5,6], where finite-time convergence for attitude stabilization was achieved in the presence of system uncertainties, external disturbances, and actuator faults. However, because passive FTC usually encompasses the upper bound of the fault, the resulting controller may be more conservative and less energy efficient.

In active FTC, an effective fault detection and identification (FDI) scheme is required to provide information about the fault with minimal uncertainties in a timely manner. Based on the estimated information, the existing controller is reconfigured to achieve system stability and desired performance. In [7], a second-order sliding-mode observer was used to estimate the mapping of reaction-wheel faults into three principal axes. Because conventional adaptive observer-based fault identification is not able to effectively identify the time-varying fault, an iterative learning observer was proposed to estimate the fault in [8]. In [9], multiple models were used to represent different actuator faults, and then a bank of interacting Kalman filters was used to achieve fault detection, isolation, and diagnosis. However, most of the aforementioned work was dedicated to the fault detection and identification for the mapped torque along the three principal axes. These FDI approaches may result in limited reconfiguration capabilities because satellite attitude control systems are usually overactuated by redundant actuators. In [10,11], local FDI algorithms were designed for each actuator to effectively reconfigure the controller, but only loss of effectiveness fault in the actuators was considered.

In [12], an active FTC scheme was proposed for spacecraft with actuator failures, where fast and accurate actuator failure detection and identification, as well as convergence of tracking errors to zero, could be guaranteed. In [13], the problem of nonlinear fault detection, isolation, and recovery for a spacecraft orbital and attitude control system was investigated, where system anomalies caused by faults were associated with changes in certain parameters in the system, and a least-squares estimation technique was used to generate residuals. Based on the fault diagnosis mechanism proposed in [8], an FTC strategy was developed in [14] to achieve attitude stabilization for spacecraft with loss of effectiveness faults and external disturbances. However, only one type of actuator fault was taken into account in the aforementioned work. In [15], loss of effectiveness faults, bias faults, and disturbances were all together treated as a lumped fault that was reconstructed by using a terminal sliding-mode observer. Based on the reconstructed fault information, a fault compensation control law was proposed for spacecraft to follow the desired attitude trajectories after a finite settling time.

In this Note, the problem of active FTC for satellites with actuator faults in the presence of both system uncertainties and external disturbances is studied. The main contributions are listed as follows:

1) Unlike the existing work in [12–14], where only one type of actuator fault (loss of effectiveness fault or bias fault) was taken into account, and the work in [15], where faults and disturbances were reconstructed as a lumped fault mapping to three axes, the proposed fault identification approach in this Note can simultaneously identify two types of faults (loss of effectiveness fault and bias fault) for each individual actuator. With this fault information, it is possible to effectively carry out control allocation, especially for redundant actuator cases.

Received 5 December 2015; revision received 30 August 2016; accepted for publication 3 December 2016; published online 24 February 2017.

*Research Fellow, Centre for System Intelligence and Efficiency (EXQUISITUS), School of Electrical and Electronic Engineering.

†Professor, Centre for System Intelligence and Efficiency (EXQUISITUS), School of Electrical and Electronic Engineering; edwwang@ntu.edu.sg (Corresponding Author).

‡Ph.D. Student, Centre for System Intelligence and Efficiency (EXQUISITUS), School of Electrical and Electronic Engineering.

§Adjunct Associate Professor, Centre for System Intelligence and Efficiency (EXQUISITUS), School of Electrical and Electronic Engineering.

2) An active fault-tolerant controller is developed to achieve finite-time attitude stabilization. Different from previous work in [5,6,22], which investigated passive FTC, the developed active FTC consists of controller reconfiguration and control allocation based on the estimated fault information. Compared to the passive FTC in previous work using the upper bound of the fault, the active FTC using the estimated fault value is less conservative and more energy effective.

3) To accommodate both healthy-actuator and faulty-actuator cases, a reconfigurable control scheme consisting of fault detection, fault identification, and fault-tolerant control is proposed. For completeness, a fault detection mechanism is also developed to detect the fault in the presence of system uncertainties and external disturbances.

II. System Modeling and Problem Formulation

In this section, satellite dynamics and an actuator fault model are first introduced; then, the problem investigated in this Note is described.

A. System Dynamics

The satellite kinetics and kinematics in terms of the quaternion can be expressed as

$$J\dot{\boldsymbol{\omega}} = -\boldsymbol{\omega}^{\times}J\boldsymbol{\omega} - \boldsymbol{\omega}^{\times}M\boldsymbol{H}_{\mathrm{rw}} + \boldsymbol{\tau} + \boldsymbol{d} \tag{1}$$

$$\dot{\boldsymbol{q}}_v = \frac{1}{2}(\boldsymbol{q}_v^{\times} + q_0\boldsymbol{I}_3)\boldsymbol{\omega} \tag{2}$$

$$\dot{q}_0 = -\frac{1}{2}\boldsymbol{q}_v^T\boldsymbol{\omega} \tag{3}$$

where $J = J^T \in \mathbb{R}^{3\times3}$ denotes the positive definite inertia matrix of the satellite; $\boldsymbol{\omega} \in \mathbb{R}^3$ is the satellite angular velocity with respect to the inertial frame $\mathcal{I}$ and expressed in the body frame $\mathcal{B}$; $M \in \mathbb{R}^{3\times n}$ is the actuator distribution matrix; $\boldsymbol{H}_{\mathrm{rw}} = [H_{\mathrm{rw},1}, H_{\mathrm{rw},2}, \ldots, H_{\mathrm{rw},n}]^T \in \mathbb{R}^n$ $(n \geq 3)$ denotes the reaction-wheel momentum; $\boldsymbol{I}_3 \in \mathbb{R}^{3\times3}$ is an identity matrix; $\boldsymbol{Q} = [\boldsymbol{q}_v^T, q_0]^T \in \mathbb{R}^3 \times \mathbb{R}$ denotes the unit quaternion describing the attitude orientation of the body frame $\mathcal{B}$ with respect to the inertial frame $\mathcal{I}$; and $\boldsymbol{\tau} \in \mathbb{R}^3$ and $\boldsymbol{d} \in \mathbb{R}^3$ denote the control torque and the external disturbances, respectively. The notation $\boldsymbol{x}^{\times} \in \mathbb{R}^{3\times3}$ for a vector $\boldsymbol{x} = [x_1, x_2, x_3]^T$ is used to represent the skew-symmetric matrix

$$\boldsymbol{x}^{\times} = \begin{bmatrix} 0 & -x_3 & x_2 \\ x_3 & 0 & -x_1 \\ -x_2 & x_1 & 0 \end{bmatrix} \tag{4}$$

Assumption 1: There exists a modeling uncertainty Δ in the satellite inertia matrix J, and $J = J_0 + \Delta J$, where J_0 is the nominal inertia matrix of the satellite. The external disturbance $\boldsymbol{d}$ is assumed to satisfy $\|\boldsymbol{d}\| \leq \gamma_d$, where γ_d is a positive constant.

Remark 1: Due to the fuel consumption and payload deployment, there may exist uncertain satellite inertia [3,16]. For a satellite attitude control system, external disturbance sources mainly include gravitation, solar radiation, magnetic forces, and aerodynamic drags.

B. Actuator Model

In this Note, reaction wheels are used as the actuators to generate control torques for satellite attitude control. To completely control the satellite attitude in space, at least three reaction wheels for which the axes of rotation are non-coplanar are required. To provide system robustness and redundancy, four or more reaction wheels may be used in a practical satellite attitude control system, e.g., four reaction wheels in a pyramid configuration. The torques provided by these wheels are denoted as $u_i, (i = 1, \ldots, n)$. Then, the following relationship between the control torque $\boldsymbol{\tau}$ and u_i can be obtained:

$$\boldsymbol{\tau} = [\tau_x\tau_y\tau_z]^T = M[u_1, \ldots, u_n]^T \tag{5}$$

For simplicity, denote $\boldsymbol{u} = [u_1, \ldots, u_n]^T$. It should be noted that the distribution matrix M is not square and has full row rank. To distribute the control torque $\boldsymbol{\tau}$ to each reaction wheel, the Moore–Penrose pseudoinverse $M^+ = M^T(MM^T)^{-1}$ is introduced. Then, given the control torque $[\tau_x, \tau_y, \tau_z]^T$, it can be derived that

$$\boldsymbol{u} = M^+[\tau_x, \tau_y, \tau_z]^T \tag{6}$$

For a healthy-actuation system, the actual output torque is equal to the command input, i.e., $\boldsymbol{u} = \boldsymbol{u}_c$. However, actuator faults are usually inevitable for many in-orbit satellites. In this Note, two types of actuator faults are considered [17]: namely, loss of actuator effectiveness and additive bias fault. These faults can be modeled as follows:

$$\boldsymbol{u} = \boldsymbol{E}\boldsymbol{u}_c + \bar{\boldsymbol{u}} \tag{7}$$

where $\boldsymbol{u}_c = [u_{c,1}, \ldots, u_{c,n}]^T$ denotes the command input of actuators, $E = \mathrm{diag}(e_1, \ldots, e_n)$ with $0 \leq e_i \leq 1$ $(i = 1, \ldots, n)$ represents the effectiveness of actuators, and $\bar{\boldsymbol{u}} \in \mathbb{R}^n$ represents the actuator bias fault. As a result, a satellite attitude kinetics model with actuator faults can be rewritten as follows:

$$J\dot{\boldsymbol{\omega}} = -\boldsymbol{\omega}^{\times}J\boldsymbol{\omega} - \boldsymbol{\omega}^{\times}M\boldsymbol{H}_{\mathrm{rw}} + M(\boldsymbol{E}\boldsymbol{u}_c + \bar{\boldsymbol{u}}) + \boldsymbol{d} \tag{8}$$

To detect and identify the actuator faults, the following actuator dynamics model is used:

$$\dot{H}_{\mathrm{rw},i} = J_{\mathrm{rw}}\dot{\Omega}_i = -u_i, \qquad i = 1, \ldots, n \tag{9}$$

where J_{rw} is the inertia of each reaction wheel, and Ω_i is the angular velocity of the ith reaction wheel. It is worth noting that the response of the reaction-wheel output torque u_i to a torque command $u_{c,i}$ is not instantaneous due to reaction-wheel friction and internal control loops, even in the healthy-actuator case. However, reaction-wheel friction can be considered as an actuator fault [defined in Eq. (7)], and the dynamics of the internal control loops is much faster than the satellite attitude dynamics. Thus, the transient response of the reaction-wheel output torque to the torque command is ignored in this Note.

C. Problem Statement

In general, satellites are designed to operate in orbit for a long lifetime during which actuator faults may occur. Once some faults occur in actuators, an FTC strategy is required to guarantee the stability and maintain attitude control performance. As compared to passive FTC, active FTC can achieve better system performance and be more energy efficient because it reconfigures the controller to accommodate the actuator faults using the estimated fault information. In this Note, the following three research issues need to be addressed for the active FTC strategy: a fault detection mechanism that is insensitive to system uncertainties and external disturbances, fault identification in the presence of multiple faults occurring in actuators, and a fault-tolerant controller.

III. Fault Detection and Identification

A. Fault Detection

This section discusses a fault detection approach that detects a fault promptly once it occurs.

Assumption 2: During fault detection, satellite angular velocities are bounded; i.e., $\|\boldsymbol{\omega}\| < \gamma_\omega < +\infty$, where γ_ω is a positive constant.

Remark 2: When all actuators are healthy, the designed attitude controller should guarantee that system states can follow the desired trajectory. Therefore, the upper bound of the angular velocity can be obtained in advance. If the angular velocity exceeds the upper bound, the fault is detected. However, in many faulty-actuator cases, the angular velocity will not exceed the upper bound for a long time,

which may result in a large attitude error. This Note will study fault detection for these faulty-actuator cases with Assumption 2.

To detect the fault, the following observer is introduced:

$$J_0\dot{\hat{\boldsymbol{\omega}}} = -\boldsymbol{\omega}^{\times}J_0\boldsymbol{\omega} - \boldsymbol{\omega}^{\times}M\boldsymbol{H}_{rw} + \boldsymbol{\tau}_c + L(\boldsymbol{\omega} - \hat{\boldsymbol{\omega}}) \tag{10}$$

where $\hat{\boldsymbol{\omega}}$ is the estimated satellite angular velocity with $\hat{\boldsymbol{\omega}}(t_0) = \boldsymbol{\omega}(t_0)$, $\boldsymbol{\tau}_c = [\tau_{c,x}, \tau_{c,y}, \tau_{c,z}]^T = M\boldsymbol{u}_c$ is the three-axis torque command, and $L \in \mathbb{R}^{3\times3}$ is a positive definite gain matrix. Let $\tilde{\boldsymbol{\omega}} = \boldsymbol{\omega} - \hat{\omega}$; comparing the satellite dynamics [Eq. (1)] with the observer [Eq. (10)] leads to

$$\begin{aligned}\dot{\tilde{\boldsymbol{\omega}}} &= -(J^{-1} - J_0^{-1})(\boldsymbol{\omega}^{\times}J_0\boldsymbol{\omega} + \boldsymbol{\omega}^{\times}M\boldsymbol{H}_{\mathrm{rw}}) - J_0^{-1}\boldsymbol{\omega}^{\times}\Delta J\omega \\ &\quad + \boldsymbol{\tau} - \tau_c - L\tilde{\boldsymbol{\omega}} + \boldsymbol{d} \\ &= (J^{-1}\Delta J J_0^{-1})(\boldsymbol{\omega}^{\times}J_0\boldsymbol{\omega} + \boldsymbol{\omega}^{\times}M\boldsymbol{H}_{\mathrm{rw}}) - J_0^{-1}\boldsymbol{\omega}^{\times}\Delta\boldsymbol{J}\boldsymbol{\omega} \\ &\quad + \boldsymbol{\tau} - \boldsymbol{\tau}_c - L\tilde{\boldsymbol{\omega}} + \boldsymbol{d}\end{aligned} \tag{11}$$

From Eq. (11), it can be known that the angular velocity estimation error depends on the uncertainties, external disturbances, and actuator faults. To use this estimation error for fault detection, it is necessary to determine the detection threshold for $\|\tilde{\boldsymbol{\omega}}\|$. According to Assumptions 1 and 2, there exists a positive constant δ such that

$$\begin{aligned}&\|(J^{-1}\Delta J J_0^{-1})(\boldsymbol{\omega}^{\times}J_0\boldsymbol{\omega} + \boldsymbol{\omega}^{\times}M\boldsymbol{H}_{\mathrm{rw}}) - J_0^{-1}\boldsymbol{\omega}^{\times}\Delta J\boldsymbol{\omega} + \boldsymbol{d}\| \\ &\quad \le \delta(1 + \gamma_\omega + \gamma_\omega^2)\end{aligned}$$

Then, the following theorem can be obtained:

Theorem 1: If there is no actuator fault occurring in the attitude control system, the angular velocity estimation error satisfies

$$\|\tilde{\boldsymbol{\omega}}\| \le \frac{\delta(1 + \gamma_\omega + \gamma_\omega^2)}{\lambda_{\min}(L)}$$

where $\lambda_{\min}(\cdot)$ denotes the minimum eigenvalue of the matrix.

Proof: Consider the following function:

$$V = \frac{1}{2}\tilde{\boldsymbol{\omega}}^T\tilde{\boldsymbol{\omega}} \tag{12}$$

Differentiating function (12) with respect to time yields

$$\dot{V} = \tilde{\boldsymbol{\omega}}^T\dot{\tilde{\boldsymbol{\omega}}} \le \|\tilde{\boldsymbol{\omega}}\|\delta(1 + \gamma_\omega + \gamma_\omega^2) + \|\tilde{\boldsymbol{\omega}}^T(\boldsymbol{\tau} - \boldsymbol{\tau}_c)\| - \lambda_{\min}(L)\|\tilde{\boldsymbol{\omega}}\|^2 \tag{13}$$

If there is no actuator fault occurring in the attitude control system, $\boldsymbol{\tau} - \boldsymbol{\tau}_c = 0$. From Eq. (13), it can be obtained that

$$\dot{V} \le \|\tilde{\boldsymbol{\omega}}\|\delta(1 + \gamma_\omega + \gamma_\omega^2) - \lambda_{\min}(L)\|\tilde{\boldsymbol{\omega}}\|^2 \tag{14}$$

It can be observed that, when

$$\|\tilde{\boldsymbol{\omega}}\| > \frac{\delta(1 + \gamma_\omega + \gamma_\omega^2)}{\lambda_{\min}(L)}, \quad \dot{V} < 0$$

With the initial condition $\hat{\boldsymbol{\omega}}(t_0) = \boldsymbol{\omega}(t_0)$, it can be concluded that

$$\|\tilde{\boldsymbol{\omega}}\| \le \frac{\delta(1 + \gamma_\omega + \gamma_\omega^2)}{\lambda_{\min}(L)}$$

for all time.

Due to the existence of uncertainties and disturbances, it is clear that, even in the healthy-actuator case, there still exists an angular velocity estimation error. Theorem 1 indicates that, for the healthy-actuator case, the angular velocity estimation error can be upper bounded by

$$\frac{\delta(1 + \gamma_\omega + \gamma_\omega^2)}{\lambda_{\min}(L)}$$

which depends on the upper bounds of uncertainties and disturbances. If a fault occurs, $\boldsymbol{\tau} - \boldsymbol{\tau}_c \neq 0$ and

$$\|\tilde{\boldsymbol{\omega}}\| \in \left[0, \frac{\delta(1 + \gamma_\omega + \gamma_\omega^2) + \|\boldsymbol{\tau} - \boldsymbol{\tau}_c\|}{\lambda_{\min}(L)}\right]$$

which implies that $\|\tilde{\boldsymbol{\omega}}\|$ may exceed the healthy-actuator bound

$$\frac{\delta(1 + \gamma_\omega + \gamma_\omega^2)}{\lambda_{\min}(L)}$$

Therefore, we can define $\|\tilde{\boldsymbol{\omega}}\|$ as the detection residual and set

$$\theta \ge \frac{\delta(1 + \gamma_\omega + \gamma_\omega^2)}{\lambda_{\min}(L)}$$

as the threshold for the detection residual. According to Theorem 1, it is clear that $\|\tilde{\boldsymbol{\omega}}\| > \theta$ indicates the occurrence of faults. It is worth noting that the threshold condition is a sufficient condition to indicate the occurrence of actuator fault; i.e., once the residual exceeds the threshold, there must be a fault or faults occurring in actuators. However, if the fault is very small, $\|\tilde{\boldsymbol{\omega}}\|$ may be lower than the selected threshold, and such a fault may not be detected.

B. Fault Identification

After the fault is detected, fault identification is activated to estimate the fault. For each reaction wheel, a local fault identification mechanism is developed. For the sake of simplicity, the subscript in Eq. (9) is dropped. The dynamics model of the reaction wheel is as follows:

$$\dot{H}_{\mathrm{rw}} = J_{\mathrm{rw}}\dot{\Omega} = -u = -eu_c - \bar{u} \tag{15}$$

To estimate the fault, the past reaction-wheel angular velocity and command input are used. Here, Ω_T and u_{cT} denote the angular velocity difference and command input difference between the time $t_1 = t - T$ $(T > 0)$ and the time $t_2 = t$, respectively, i.e., $\Omega_T = \Omega(t) - \Omega(t - T)$ and $u_{cT} = u_c(t) - u_c(t - T)$. The dynamics of Ω_T is derived as follows:

$$J_{\mathrm{rw}}\dot{\Omega}_T = -eu_{cT} \tag{16}$$

Now, we proceed to design the adaptive observers for the fault identification as follows:

$$J_{\mathrm{rw}}\dot{\hat{\Omega}} = -\hat{e}u_c - \hat{\bar{u}} + l_1\tilde{\Omega} \tag{17}$$

$$J_{\mathrm{rw}}\dot{\hat{\Omega}}_T = -\hat{e}u_{cT} + l_2\tilde{\Omega}_T \tag{18}$$

where l_1 and l_2 are positive constants; $\tilde{\Omega} = \Omega - \hat{\Omega}$; $\tilde{\Omega}_T = \Omega_T - \hat{\Omega}_T$, and $\hat{e}$ and $\hat{\bar{u}}$ are the estimates of effectiveness and bias, respectively. With the reaction-wheel dynamic models and observers (15–18), the estimation error dynamics can be calculated as follows:

$$J_{\mathrm{rw}}\dot{\tilde{\Omega}} = -\tilde{e}u_c - \tilde{\bar{u}} - l_1\tilde{\Omega} \tag{19}$$

$$J_{\mathrm{rw}}\dot{\tilde{\Omega}}_T = -\tilde{e}u_{cT} - l_2\tilde{\Omega}_T \tag{20}$$

where $\tilde{e} = e - \hat{e}$ and $\tilde{\bar{u}} = \bar{u} - \hat{\bar{u}}$. To ensure the estimates to be bounded, the following transformation is applied:

$$e = C_1(\tanh(\phi_1) + 1), \qquad \bar{u} = C_2\tanh(\phi_2) \tag{21}$$

$$\hat{e} = C_1(\tanh(\hat{\phi}_1) + 1), \qquad \hat{\tilde{u}} = C_2 \tanh(\hat{\phi}_2) \tag{22}$$

where C_1 and C_2 are positive constants that determine the bounds of the estimates, ϕ_1 and ϕ_2 are transformed effectiveness and bias, $\hat{\phi}_1$ and $\hat{\phi}_2$ are two adaptive variables, and

$$\tanh(x) = \frac{e^x - e^{-x}}{e^x + e^{-x}}$$

Then, it can be derived from Eqs. (21) and (22) that

$$\tilde{e} = C_1(\tanh(\phi_1) - \tanh(\hat{\phi}_1)) \tag{23}$$

$$\tilde{\tilde{u}} = C_2(\tanh(\phi_2) - \tanh(\hat{\phi}_2)) \tag{24}$$

The adaptive update laws are designed as follows:

$$\dot{\hat{\phi}}_1 = -\eta_1 u_c \tilde{\Omega} - \eta_1 u_{cT} \tilde{\Omega}_T \tag{25}$$

$$\dot{\hat{\phi}}_2 = -\eta_2 \tilde{\Omega} \tag{26}$$

where η_1 and η_2 are positive constants that determine the convergence rate. Based on the aforementioned analysis, the following theorem can be obtained.

Theorem 2: Considering the actuator models (15) and (16) with unknown effectiveness e and bias $\bar{u}$, two adaptive observers are designed as Eqs. (17) and (18) with adaptive variables defined in Eq. (22) and adaptive update laws (25) and (26). If u_c and u_{cT} are bounded and uniformly continuous, and u_{cT} is not identically zero, the fault estimation errors will asymptotically converge to zero, i.e., $\lim_{t\to\infty} \tilde{e} = 0$ and $\lim_{t\to\infty} \tilde{\tilde{u}} = 0$.

Proof: Consider the Lyapunov function candidate

$$V = \frac{1}{2} J_{\text{rw}} \tilde{\Omega}^2 + \frac{1}{2} J_{\text{rw}} \tilde{\Omega}_T^2 + \frac{C_1}{\eta_1}\left(\log\ \cosh(\hat{\phi}_1) - \hat{\phi}_1 \tanh(\phi_1)\right) + \frac{C_2}{\eta_2}\left(\log\ \cosh(\hat{\phi}_2) - \hat{\phi}_2 \tanh(\phi_2)\right) + C \tag{27}$$

where C is a positive constant that is used to ensure that $V \geq 0$.

Differentiating function (27) with respect to time leads to

$$\begin{aligned}\dot{V} &= -\tilde{\Omega}(\tilde{e}u_c + \tilde{\tilde{u}} + l_1\tilde{\Omega}) - \tilde{\Omega}_T(\tilde{e}u_{cT} + l_2\tilde{\Omega}_T) \\ &\quad - \frac{\dot{\hat{\phi}}_1}{\eta_1} C_1\left(\tanh(\phi_1) - \tanh(\hat{\phi}_1)\right) - \frac{\dot{\hat{\phi}}_2}{\eta_2} C_2\left(\tanh(\phi_2) - \tanh(\hat{\phi}_2)\right) \\ &= -\tilde{\Omega}(\tilde{e}u_c + \tilde{\tilde{u}} + l_1\tilde{\Omega}) - \tilde{\Omega}_T(\tilde{e}u_{cT} + l_2\tilde{\Omega}_T) - \frac{\dot{\hat{\phi}}_1}{\eta_1}\tilde{e} - \frac{\dot{\hat{\phi}}_2}{\eta_2}\tilde{\tilde{u}}\end{aligned} \tag{28}$$

Substituting Eqs. (25) and (26) into Eq. (28) results in

$$\dot{V} = -l_1\tilde{\Omega}^2 - l_2\tilde{\Omega}_T^2 \leq 0 \tag{29}$$

From Eqs. (27) and (29), it can be obtained that $0 \leq V \leq V(0)$ and $\dot{V} \leq 0$, so $\tilde{\Omega}$ and $\tilde{\Omega}_T$ are bounded. Because $\tilde{e}$ and $\tilde{\tilde{u}}$ are bounded, it can also be noted from Eqs. (19) and (20) that $\tilde{\Omega}$ and $\tilde{\Omega}_T$ are bounded. Therefore, $\ddot{V} = -l_1\tilde{\Omega}\dot{\tilde{\Omega}} - l_2\tilde{\Omega}_T\dot{\tilde{\Omega}}_T$ is bounded as well. According to Barbalat's lemma, $\lim_{t\to\infty} \dot{V} = 0$ which in turn implies that $\lim_{t\to\infty} \tilde{\Omega} = 0$ and $\lim_{t\to\infty} \tilde{\Omega}_T = 0$.

Differentiating $J_{\text{rw}}\tilde{\Omega}$ and $J_{\text{rw}}\tilde{\Omega}_T$ with respect to time yields

$$J_{\text{rw}}\ddot{\tilde{\Omega}} = \dot{\hat{e}}u_c - \tilde{e}\dot{u}_c + \dot{\tilde{\tilde{u}}} - l_1\dot{\tilde{\Omega}} \tag{30}$$

$$J_{\text{rw}}\ddot{\tilde{\Omega}}_T = \dot{\hat{e}}u_{cT} - \tilde{e}\dot{u}_{cT} - l_2\dot{\tilde{\Omega}}_T \tag{31}$$

According to the definitions of $\hat{e}$ and $\hat{\tilde{u}}$,

$$\dot{\hat{e}} = C_1\dot{\hat{\phi}}_1 \frac{\partial \tanh(\hat{\phi}_1)}{\partial \hat{\phi}_1} = \frac{C_1\dot{\hat{\phi}}_1}{(e^{\hat{\phi}_1} + e^{-\hat{\phi}_1})^2}$$

and

$$\dot{\hat{\tilde{u}}} = C_2\dot{\hat{\phi}}_2 \frac{\partial \tanh(\hat{\phi}_2)}{\partial \hat{\phi}_2} = \frac{C_2\dot{\hat{\phi}}_2}{(e^{\hat{\phi}_2} + e^{-\hat{\phi}_2})^2}$$

As u_c, u_{cT}, $\dot{u}_c$, and $\dot{u}_{cT}$ are bounded, with adaptive laws (25) and (26), it can be obtained that $\hat{e}$ and $\hat{\tilde{u}}$ are also bounded. Therefore, it can be observed from Eqs. (30) and (31) that $\dot{\tilde{\Omega}}$ and $\dot{\tilde{\Omega}}_T$ are bounded. According to Barbalat's lemma, it is concluded that $\lim_{t\to\infty}\dot{\tilde{\Omega}} = 0$ and $\lim_{t\to\infty}\tilde{\Omega}_T = 0$. Because u_{cT} is not identically zero, from Eq. (20), it is clear that $\lim_{t\to\infty}\tilde{e} = 0$. Then, from Eq. (19), it is derived that $\lim_{t\to\infty}\tilde{\tilde{u}} = 0$. Hence, the fault estimates asymptotically converge to the true values.

Remark 3: Due to the asymptotical convergence property, it may take a very long time for the estimates to converge to the true values. Thus, there is a tradeoff between identification time and estimation accuracy. The angular velocity estimation error of the reaction wheel and the variation of the fault estimates are combined to generate a residual δ_{id} as follows:

$$\delta_{id} = \frac{1}{T_0}\int_{t_c - T_0}^{t_c} (\|\tilde{\Omega}(t)\| + \|\tilde{\Omega}_T(t)\| + \|\hat{e}(t) - \hat{e}(t - T_1)\| + \|\hat{\tilde{u}}(t) - \hat{\tilde{u}}(t - T_1)\|)\,\mathrm{d}t \tag{32}$$

where t_c denotes the current time, and T_0 and T_1 are positive constants. If this residual is smaller than the given threshold, it is concluded the fault identification is completed. It is noted that the smaller the threshold is set, the more accurate the fault estimates.

IV. Fault-Tolerant Control Design

In this section, the overall active fault-tolerant control scheme is studied. To enhance the reliability, maneuverability, and survivability, the satellite attitude control system generally uses redundant actuators. Thus, satellite attitude control design consists of two parts: the reconfigurable controller and control allocation. As a high-level controller, the reconfigurable controller is designed to generate torque command along three axes, whereas control allocation is used as a low-level controller to distribute this torque command to each actuator. When a fault occurs in an actuator, the faulty actuator may not be able to provide the distributed command torque, which may lead to system performance degradation. Therefore, FDI and/or controller reconfiguration are required to ensure the system performance.

Based on the proposed fault detection and identification mechanism, the overall proposed fault-tolerant control scheme is shown in Fig. 1. As depicted in Fig. 1, $\boldsymbol{Q}_d$ and $\boldsymbol{\omega}_d$ are the desired satellite attitude and angular velocity, respectively; $\boldsymbol{\tau}_c$ denotes the three-axis control torque command generated by the reconfigurable controller; $\boldsymbol{u}_c$ is the command input to reaction wheels generated by the control allocation; and $\hat{\boldsymbol{E}}$ and $\hat{\tilde{\boldsymbol{u}}}$ are the estimated effectiveness and bias, respectively. The reconfigurable controller consists of three controllers: basic controller, passive FTC, and active FTC. When no fault is detected, the basic controller is used. As shown in Fig. 1, switching signal 1 denotes that the fault is detected. Once a fault is detected, fault identification is activated to estimate the fault; meanwhile, the reconfigurable controller is switched to passive FTC in order to guarantee the system performance. During this period, because the reaction-wheel fault has not been identified, control allocation uses the pseudoinverse of M to generate control input for each reaction wheel. Switching signal 2 denotes that the fault identification is completed. After the fault is identified, the reconfigurable controller is switched to active FTC and the estimated effectiveness and bias fault are used for control allocation. Next, the controller reconfiguration and control allocation approaches are discussed.

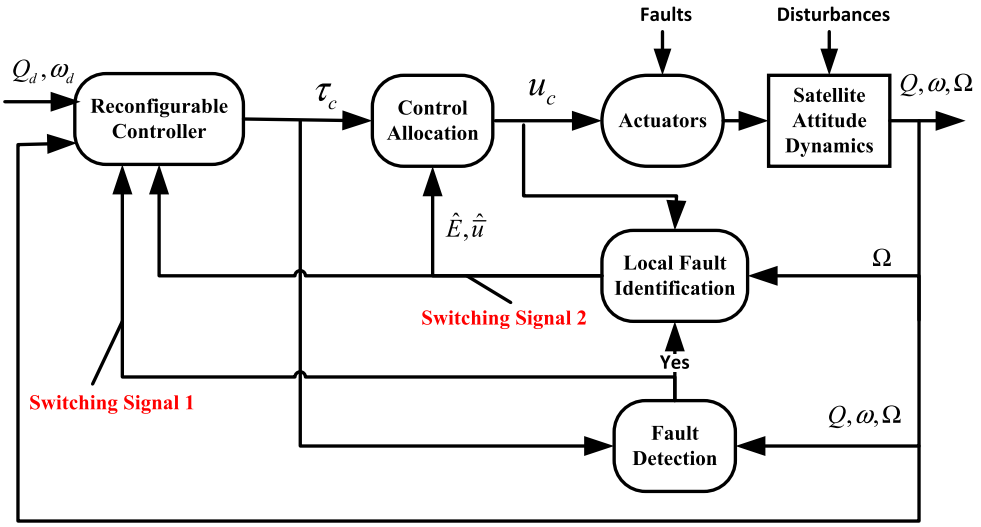

Fig. 1 Overall fault-tolerant control scheme.

A. Transformed Attitude Dynamics and Sliding-Mode Manifold

To address the attitude stabilization problem, the satellite attitude dynamics is rewritten by using a Lagrange-like equation [6,18,19]. Let

$$\boldsymbol{P} = \left[\frac{1}{2}(\boldsymbol{q}_v^{\times} + q_0 \boldsymbol{I}_3)\right]^{-1} \in \mathbb{R}^{3\times 3}$$

and then attitude dynamics (1) can be rewritten as follows:

$$J^*\ddot{\boldsymbol{q}}_v = -\boldsymbol{\Xi}\dot{\boldsymbol{q}}_v + \boldsymbol{P}^T M \boldsymbol{H}_{\text{rw}}^{\times}\boldsymbol{P}\dot{\boldsymbol{q}}_v + \boldsymbol{P}^T\boldsymbol{\tau} + \boldsymbol{T}_d \tag{33}$$

where $J^* = \boldsymbol{P}^T J_0 \boldsymbol{P}$, $\boldsymbol{\Xi} = \boldsymbol{P}^T J_0 \dot{\boldsymbol{P}} - \boldsymbol{P}^T (J_0 \boldsymbol{P}\dot{\boldsymbol{q}}_v)^{\times}\boldsymbol{P}$, and $\boldsymbol{T}_d = \boldsymbol{P}^T(\boldsymbol{d}(t) - \Delta J\dot{\omega} - \boldsymbol{\omega}^{\times}\Delta J\boldsymbol{\omega})$. $\boldsymbol{T}_d$ is considered as the lumped disturbances and uncertainties. According to Assumption 1, there exists a positive constant γ_0 such that $\|\boldsymbol{T}_d\| \le \gamma_0 W$, where $W = 1 + \|\boldsymbol{\omega}\| + \|\boldsymbol{\omega}\|^2$.

To design the control scheme, a finite-time sliding-mode manifold (proposed in [6]) is used. The sliding-mode manifold $\boldsymbol{s} \in \mathbb{R}^3$ is defined as

$$\boldsymbol{s} = \dot{\boldsymbol{q}}_v + \boldsymbol{\alpha}\boldsymbol{q}_v + \boldsymbol{\beta}\text{sig}(\boldsymbol{q}_v)^r \tag{34}$$

where $\alpha = \text{diag}(\alpha_1, \alpha_2, \alpha_3)$ and $\boldsymbol{\beta} = \text{diag}(\beta_1, \beta_2, \beta_3)$ are positive definite and diagonal matrices, r is a positive constant satisfying $0 < r < 1$, and $\text{sig}(\cdot)$ is defined as

$$\text{sig}(\boldsymbol{q}_v)^r = [|q_{v,1}|^r \text{sign}(q_{v,1}) |q_{v,2}|^r \text{sign}(q_{v,2}) |q_{v,3}|^r \text{sign}(q_{v,3})]^T \tag{35}$$

where $q_{v,j}$ is the jth component of $\boldsymbol{q}_v$, $j = 1, 2$, and 3. To avoid singularity, $\dot{\boldsymbol{s}}$ is modified as [20]

$$\dot{\boldsymbol{s}} = \ddot{\boldsymbol{q}}_v + \boldsymbol{\alpha}\dot{\boldsymbol{q}}_v + \boldsymbol{\beta}\boldsymbol{q}_{vr} \tag{36}$$

with $\boldsymbol{q}_{vr} \in \mathbb{R}^3$ defined as

$$q_{vr,j} = \begin{cases} r|q_{v,j}|^{r-1}\dot{q}_{v,j} & \text{if } |q_{v,j}| \ge \epsilon, \quad \text{and} \quad \dot{q}_{v,j} \ne 0 \\ r|\epsilon|^{r-1}\dot{q}_{v,j} & \text{if } |q_{v,j}| < \epsilon, \quad \text{and} \quad \dot{q}_{v,j} \ne 0 \\ 0 & \text{if } \dot{q}_{v,j} = 0 \end{cases}$$

where ϵ is a small positive constant. Applying the sliding-mode manifold [Eq. (34)] into Eq. (33) results in

$$J^*\dot{\boldsymbol{s}} = -\boldsymbol{\Xi}\boldsymbol{s} + \boldsymbol{P}^T\boldsymbol{\tau} + \boldsymbol{F} + \boldsymbol{T}_d \tag{37}$$

where

$$\boldsymbol{F} = \boldsymbol{P}^T M \boldsymbol{H}_{\text{rw}}^{\times}\boldsymbol{P}\dot{\boldsymbol{q}}_v + \boldsymbol{\Xi}\boldsymbol{\alpha}\boldsymbol{q}_v + \boldsymbol{\Xi}\boldsymbol{\beta}\text{sig}(\boldsymbol{q}_v)^r + J^*\boldsymbol{\alpha}\dot{\boldsymbol{q}}_v + J^*\boldsymbol{\beta}\boldsymbol{q}_{vr}$$

According to the property of the finite-time sliding-mode manifold, the following lemma can be obtained:

Lemma 1 [5]: Consider the terminal sliding-mode manifold $\boldsymbol{s}$ defined by Eq. (34). If the sliding-mode manifold satisfies $\boldsymbol{s} = 0$, then the equilibrium point $\boldsymbol{q}_v = 0$ is globally finite-time stable, i.e., the system state $\boldsymbol{q}_v$ that starts from $\boldsymbol{q}_v(0)$ converges to $\boldsymbol{q}_v = 0$ in finite time.

B. Basic Controller and Passive FTC Design

In this section, the basic controller for the healthy-actuator case and the passive FTC controller for the faulty-actuator case are designed. The following assumptions are required:

Assumption 3: The additive fault introduced in fault model (7) satisfies

$$\|\bar{\boldsymbol{u}}\| \le f_0 \tag{38}$$

where f_0 is a positive constant.

Assumption 4 [3]: Matrix $\boldsymbol{MEM}^T$ is positive definite, and

$$0 < e_0 \le \min\{\lambda_{\min}(\boldsymbol{MEM}^T), 1\} \tag{39}$$

where e_0 is a positive constant.

Remark 4: Assumption 4 means that, although some actuators may suffer from partial loss of actuator effectiveness or even complete failure, the combination of all actuators should still guarantee that $\boldsymbol{MEM}^T$ remains positive definite.

To reject system uncertainties and external disturbances with healthy actuators, the basic controller is designed as follows:

$$\tau_c = \boldsymbol{\tau}_{\text{basic}} = -\boldsymbol{P}^{-T}[\boldsymbol{k}_1\boldsymbol{s} + \boldsymbol{k}_2\text{sig}(\boldsymbol{s})^{\rho} + \|\boldsymbol{F}\|\text{sign}(\boldsymbol{s}) + \gamma_0 W\text{sign}(\boldsymbol{s})] \tag{40}$$

where $\boldsymbol{k}_1 = \text{diag}(k_{1,1}, k_{1,2}, k_{1,3})$ and $\boldsymbol{k}_2 = \text{diag}(k_{2,1}, k_{2,2}, k_{2,3})$ are two positive definite matrices, and ρ is a positive constant satisfying $0 < \rho < 1$.

Based on this controller, the command torque for each reaction wheel can be obtained by using Eq. (6). Because there is no fault occurring in actuators, it is clear that $\boldsymbol{E} = \boldsymbol{I}_n$ and $\bar{\boldsymbol{u}} = 0$ so that $\boldsymbol{\tau} = \boldsymbol{\tau}_c$. Define the Lyapunov function candidate as

$$V_1 = \frac{1}{2}s^T J^* s \tag{41}$$

Differentiating V_1 with respect to time yields that

$$\dot{V}_1 = \frac{1}{2}s^T\dot{J}^*s + s^T(-\Xi s + P^T\tau + F + T_d) \leq -s^Tk_1s - s^Tk_2\text{sig}(s)^\rho$$

It can be obtained that s converges to zero in finite time. Thus, according to Lemma 1, $\boldsymbol{q}_v \to 0$ and $\boldsymbol{\omega} \to 0$ in finite time.

After a fault occurs, the system performance may be degraded. Once the estimation error of the fault detection exceeds the detection threshold, the fault can be detected. Then, passive FTC is adopted to generate command torque for the satellite. There is plenty of work done in the literature on passive FTC, such as in [3,4,6,21,22]. In this Note, the passive FTC proposed in [6] is used:

$$\boldsymbol{\tau}_c = \boldsymbol{\tau}_{pa} = -MM^T\boldsymbol{P}^{-T}[\boldsymbol{u}_{\text{nom}} + \gamma_1\|\boldsymbol{P}^TM\|\text{sign}(\boldsymbol{s}) + \gamma_2\|\boldsymbol{u}_{\text{nom}}\|\text{sign}(\boldsymbol{s})] \tag{42}$$

where

$$\boldsymbol{u}_{\text{nom}} = \boldsymbol{k}_1\boldsymbol{s} + \boldsymbol{k}_2\text{sig}(\boldsymbol{s})^\rho + \|\boldsymbol{F}\|\text{sign}(\boldsymbol{s}) + \gamma_0 W\text{sign}(\boldsymbol{s}), \quad \gamma_1 \geq \frac{f_0}{e_0}$$

and

$$\gamma_2 \geq \frac{1}{e_0} - 1$$

For the system analysis and stability proof for the passive FTC (42), please refer to the paper in [6].

Remark 5: The proposed basic controller and passive FTC are used as the reconfigurable controller, which is a high-level controller. Because fault identification is not completed during these periods, Eq. (6) is used for control allocation.

C. Active FTC Design

Actuator faults can be estimated by the proposed fault identification approach. Once the faults are identified, this information can be used to reconfigure the controller and reallocate appropriate control torque to each reaction wheel. There may exist estimation errors in the fault information, and the estimation errors are defined as $\|\Delta\boldsymbol{E}\|$ and $\|\Delta\bar{\boldsymbol{u}}\|$ such that $\boldsymbol{E} = \hat{\boldsymbol{E}} + \Delta\boldsymbol{E}$ and $\bar{\boldsymbol{u}} = \hat{\bar{\boldsymbol{u}}} + \Delta\bar{\boldsymbol{u}}$. To design active FTC law for satellite attitude control, the following assumption is required:

Assumption 5: It is assumed that the fault estimation errors $\|\Delta\boldsymbol{E}\|$ and $\|\Delta\bar{\boldsymbol{u}}\|$ are bounded and satisfy $\|\boldsymbol{ME}[(M\hat{E})^+ - (\boldsymbol{ME})^+]\| \leq \boldsymbol{\gamma}_3$ and $\|\boldsymbol{P}^T\boldsymbol{ME}[(M\hat{E})^+ - (\boldsymbol{ME})^+]M\hat{\bar{\boldsymbol{u}}} - \boldsymbol{P}^TM\Delta\bar{\boldsymbol{u}}\| \leq \boldsymbol{\gamma}_4$.

Remark 6: If $\|\Delta\boldsymbol{E}\|/\|\boldsymbol{E}\|$ is small, $\|\boldsymbol{ME}[(M\hat{E})^+ - (\boldsymbol{ME})^+]\| \approx \|\boldsymbol{ME}(M\Delta\boldsymbol{E})^T((\boldsymbol{ME})(\boldsymbol{ME})^T)^{-1}\| \leq \gamma_E\|\Delta E\|$, where γ_E is a positive constant.

The active FTC is designed as

$$\boldsymbol{\tau}_c = \boldsymbol{\tau}_{\text{active}} = \boldsymbol{\tau}_{\text{basic}} - P^{-T}\gamma_4\text{sign}(\boldsymbol{s}) - \frac{\gamma_3}{1-\gamma_3}\|\boldsymbol{P}^T\boldsymbol{\tau}_{\text{basic}} - \gamma_4\text{sign}(\boldsymbol{s})\|\boldsymbol{P}^{-T}\text{sign}(\boldsymbol{s}) \tag{43}$$

In contrast to the basic controller and passive FTC design, active FTC takes advantage of the estimated fault information to generate the control input $\boldsymbol{u}_c$ via

$$\boldsymbol{u}_c = (M\hat{\boldsymbol{E}})^+(\boldsymbol{\tau}_c - M\hat{\bar{\boldsymbol{u}}}) \tag{44}$$

Based on the active FTC [Eq. (43)] and control allocation [Eq. (44)], the following theorem can be obtained:

Theorem 3: Consider the attitude control systems described by Eqs. (1–3) in the presence of partial loss of actuator effectiveness fault and additive fault. If Assumptions 1–5 are satisfied and the controller [Eq. (43)] and control allocation [Eq. (44)] are applied, then the states of systems (1) and (2) will be stabilized to the origin in finite time; i.e., $\boldsymbol{q}_v \to 0$ and $\boldsymbol{\omega} \to 0$ in finite time.

Proof: Consider the following Lyapunov function candidate:

$$V_2 = \frac{1}{2}s^TJ^*s \tag{45}$$

Using Eq. (37), the time derivative of V_2 is

$$\dot{V}_2 = \frac{1}{2}s^T\dot{J}^*s + s^T(-\Xi s + P^T\boldsymbol{ME}u_c + P^TM\bar{u} + F + T_d)$$

In view of the control law [Eq. (43)] and control allocation [Eq. (44)], it follows that

$$\begin{aligned}
\dot{V}_2 &= s^T\Big(P^T\boldsymbol{ME}(M\hat{E})^+(\tau_c - M\hat{\bar{u}}) + P^TM\bar{u} + F + T_d\Big)\\
&= s^T\Big(P^T(\tau_c - M\hat{\bar{u}}) + P^TM\bar{u} + F + T_d\\
&\quad + P^T\boldsymbol{ME}[(M\hat{E})^+ - (\boldsymbol{ME})^+](\tau_c - M\hat{\bar{u}})\Big)\\
&= s^T\Big(P^T(\tau_c - M\bar{u}) + P^TM\Delta\bar{u} + P^TM\bar{u} + F + T_d\\
&\quad + P^T\boldsymbol{ME}[(M\hat{E})^+ - (\boldsymbol{ME})^+](\tau_c - M\hat{\bar{u}})\Big)\\
&\leq -s^Tk_1s - s^Tk_2sig(s)^\rho - \gamma_4\|s\|\\
&\quad - \frac{\gamma_3}{1-\gamma_3}\|P^T\tau_{\text{basic}} - \gamma_4\text{sign}(s)\| \cdot \|s\|\\
&\quad + \|P^T(\boldsymbol{ME}[(M\hat{E})^+ - (\boldsymbol{ME})^+]M\hat{\bar{u}} - M\Delta\bar{u})\| \cdot \|s\|\\
&\quad + \|P^T\boldsymbol{ME}[(M\hat{E})^+ - (\boldsymbol{ME})^+]\tau_c\| \cdot \|s\|
\end{aligned}$$

According to the Assumption 5, it can be derived that

$$\begin{aligned}
\dot{V}_2 &\leq -s^Tk_1s - s^Tk_2\text{sig}(s)^\rho - \frac{\gamma_3}{1-\gamma_3}\|P^T\tau_{\text{basic}} - \gamma_4\text{sign}(s)\| \cdot \|s\|\\
&\quad + \gamma_3\|s\| \cdot \|P^T\tau_{\text{basic}} - \gamma_4\text{sign}(s)\|\left(1 + \frac{\gamma_3}{1-\gamma_3}\right)\\
&\leq -s^Tk_1s - s^Tk_2\text{sig}(s)^\rho
\end{aligned}$$

With Lemma 1, it can be concluded that the states of systems (1) and (2) will be stabilized to the origin in finite time; i.e., $\boldsymbol{q}_v \to 0$ and $\boldsymbol{\omega} \to 0$ in finite time. This completes the proof.

Remark 7: As compared with the basic controller, the active FTC [Eq. (43)] has two more terms that are used to eliminate the influence caused by fault estimation errors. If the estimation is very accurate, parameters γ_3 and γ_4 can be very small so that the active FTC is very close to the basic controller. As compared with the passive FTC, γ_3 and γ_4 should be much smaller than γ_1 and γ_2 because γ_1 and γ_2 are derived by considering the upper bounds of the faults. Therefore, the command torque generated by the proposed active FTC can be made smaller than that generated by the passive FTC.

V. Simulation

In this section, satellite attitude stabilization control with actuator faults is studied through simulation. Four reaction wheels in a

Table 1 Actuator fault scenarios

Scenario	Parameter
One (S1)	At $t = 5s$: $e_1 = 0.8$, $\bar{u}_1 = -0.03$ N · m, $e_2 = 0.6$, $\bar{u}_3 = 0.02$ N · m
Two (S2)	At $t = 5s$: $e_1 = 0.8$, $\bar{u}_3 = 0.02$ N · m, $e_2 = 0.6$ At $t = 100s$: $\bar{u}_1 = -0.03$ N · m

Table 2 FDI and FTC design parameters

Parameter	Value
L	$0.1\ \boldsymbol{I}_3$
T	2 s
θ	0.001
l_1	0.8
l_2	0.45
η_1	1200
η_2	80
C_1	0.51
C_2	0.04
α	$0.05\ \boldsymbol{I}_3$
ϵ	0.001
$\boldsymbol{\beta}$	$0.01\ \boldsymbol{I}_3$
r	0.55
e_0	0.5
f_0	0.03
h	1000
ρ	0.55
γ_3	0.01
γ_4	0.001
$\boldsymbol{k}_1$	$0.0356\ J_0$
$\boldsymbol{k}_2$	$0.2667\ J_0$

pyramid configuration are used as actuators to provide control torques. The distribution matrix M, the satellite nominal inertia matrix, and the uncertain inertia are as follows:

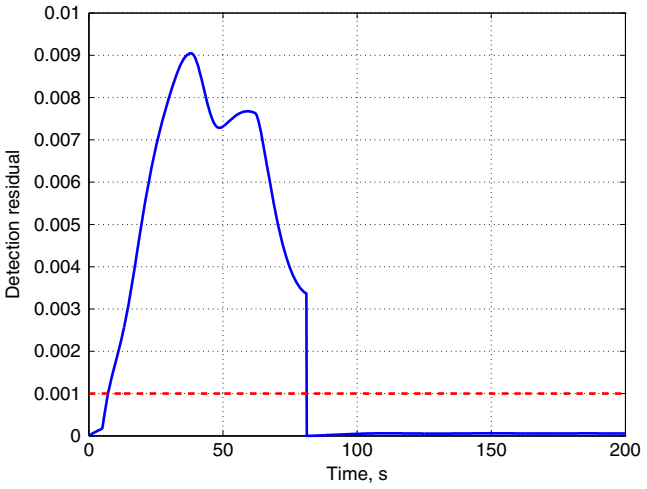

Fig. 2 Fault detection (S1).

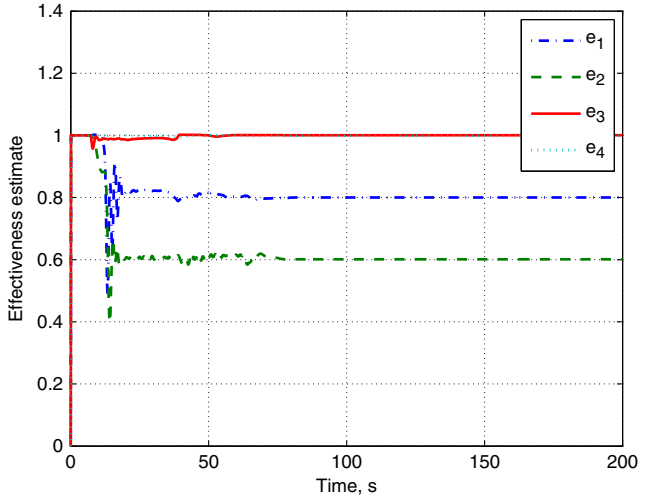

Fig. 3 Effectiveness estimation (S1).

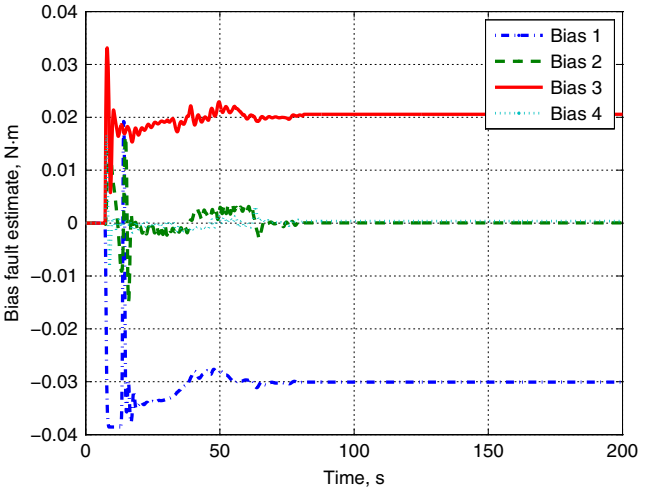

Fig. 4 Bias fault estimation (S1).

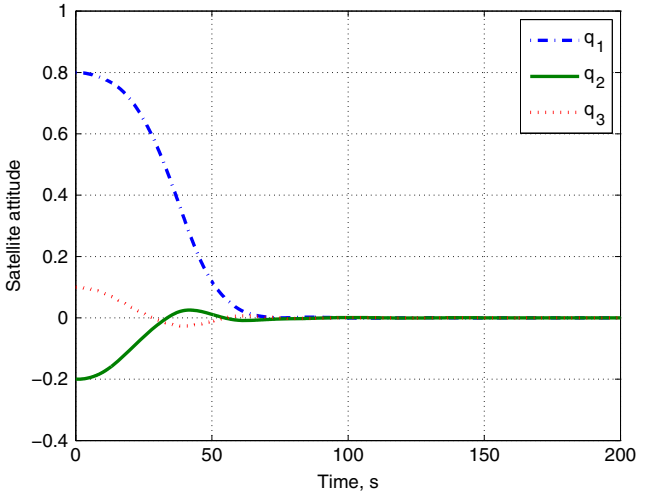

Fig. 5 Satellite attitude (S1).

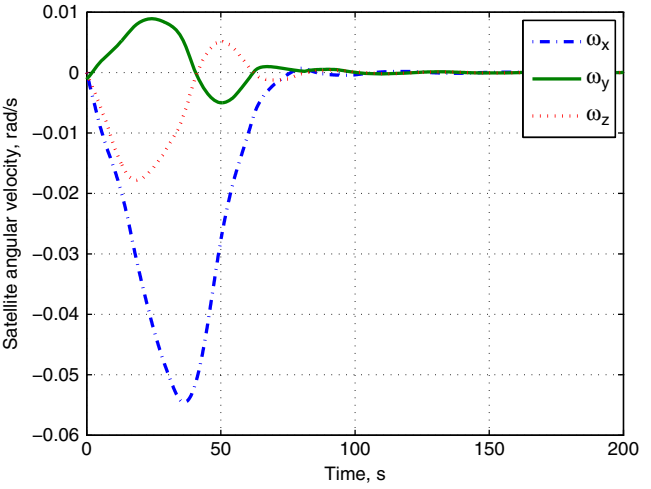

Fig. 6 Satellite angular velocity (S1).

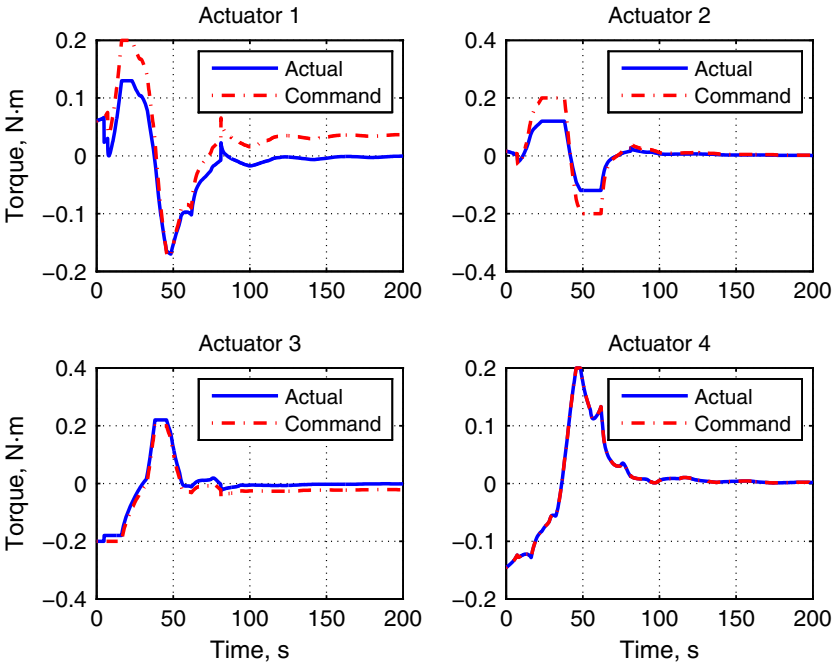

Fig. 7 Command and actual torques (S1).

$$M = \frac{1}{\sqrt{3}}\begin{bmatrix} -1 & -1 & 1 & 1 \\ 1 & -1 & -1 & 1 \\ 1 & 1 & 1 & 1 \end{bmatrix}.$$

$$J_0 = \begin{bmatrix} 130 & 6.5 & 6 \\ 6.5 & 140 & 5.5 \\ 6 & 5.5 & 135 \end{bmatrix} \text{kg} \cdot \text{m}^2,$$

$$\Delta J = \begin{bmatrix} 3 & 0 & 0 \\ 0 & 2 & 0 \\ 0 & 0 & -2.5 \end{bmatrix} \text{kg} \cdot \text{m}^2$$

The simulation consists of two fault scenarios, described in Table 1. The FDI and FTC design parameters are presented in Table 2. The initial states of the satellite are as follows: $Q_0 = [0.8, -0.2, 0.1, 0.557]$ and $\omega_0 = [0, 0.0011, 0]\text{rad/s}$. Based on the aforementioned setting, the satellite attitude control simulation is carried out to verify the proposed integrated FDI and FTC solution.

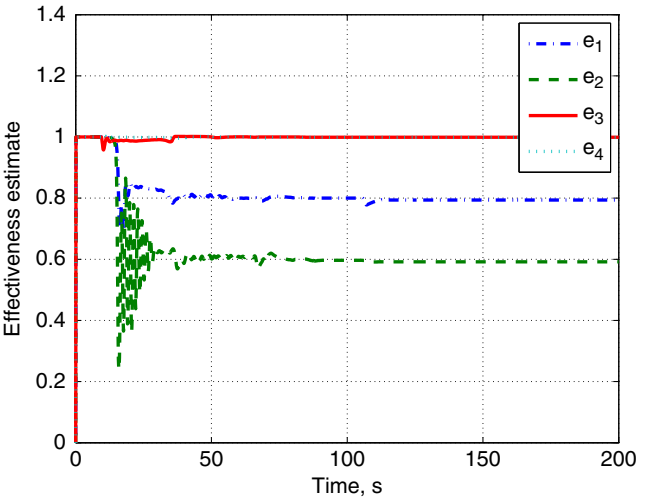

Fig. 9 Effectiveness estimation (S2).

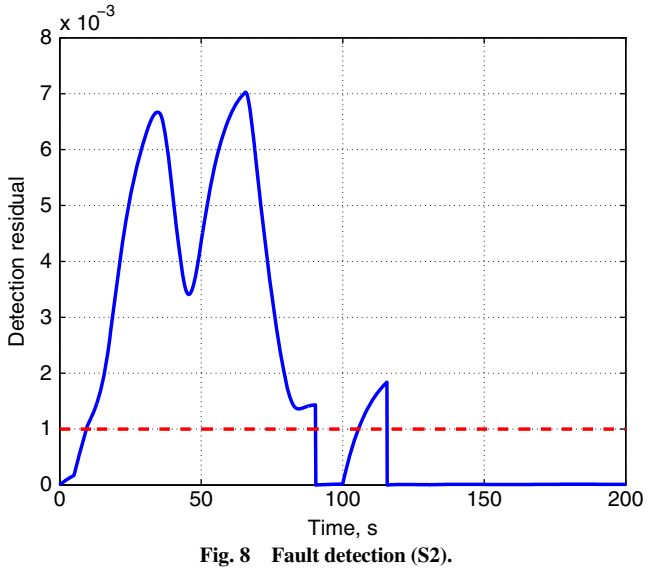

Fig. 8 Fault detection (S2).

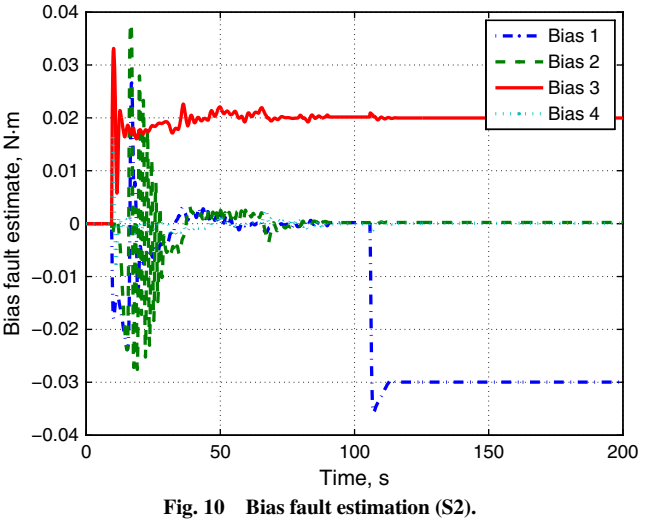

Fig. 10 Bias fault estimation (S2).

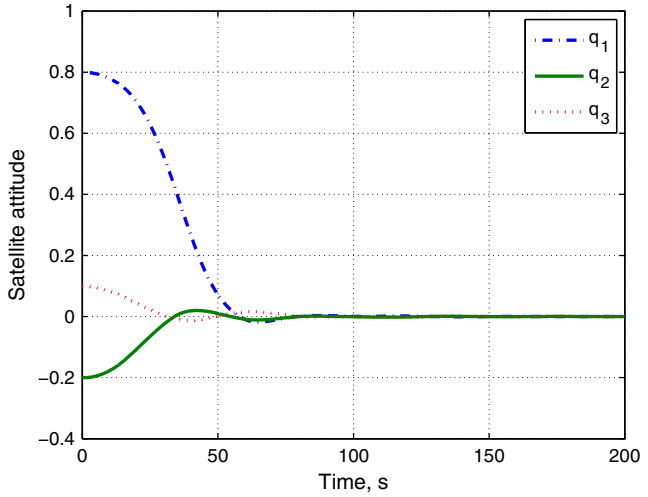

Fig. 11 Satellite attitude (S2).

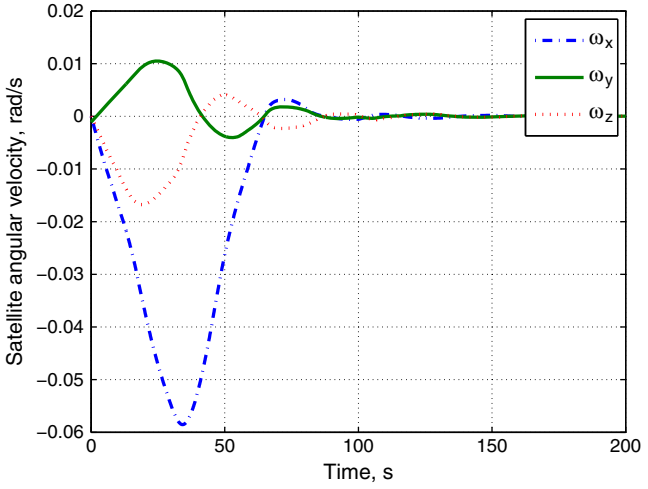

Fig. 12 Satellite angular velocity (S2).

A. Scenario One

In scenario one, it can be seen from Table 1 that all faults occur at the same time. As shown in Fig. 2, before the actuator faults occur, the fault detection residual $\|\tilde{\omega}\|$ is not equal to zero due to system uncertainties and external disturbances, but it will never exceed the threshold θ, as discussed in Theorem 1. Upon occurrence of the faults, the residual increases quickly and exceeds the threshold, i.e., the fault is detected. Then, the fault identification is activated to estimate the exact faults. It can be seen from Figs. 3 and 4 that the proposed fault identification approach can estimate the faults accurately. Because the function $\tanh(x)$ is introduced to represent the fault estimates, it can be observed that all the fault estimates during fault identification are bounded. Once the faults are identified, the fault information is used to update the controller and fault detection mechanism so that the residual goes down below the threshold, as depicted in Fig. 2. However, it is worth noting that, during attitude maneuver, the fault identification time may be limited, and thus tradeoff between estimation time and accuracy may result in an error between the estimate and the true value.

With the proposed reconfigurable controller, it can be noted from Figs. 5 and 6 that the attitude and angular velocity asymptotically converge to zero. Figure 7 shows the command and actual control torques. The dashed–dotted line represents the command torque, and the solid line represents the actual control torque provided by reaction wheels. As bias fault occurs in reaction wheels one and three, the difference between the command torque and the actual torque always exists. In contrast, a loss of effectiveness fault occurs in reaction wheel two, but the actual torque is almost equal to the command when the command torque is small. Therefore, when command torque is very small, it may be impossible to detect and identify the loss of effectiveness fault.

B. Scenario Two

In this section, the case with fault scenario two is studied by simulation. As shown in Fig. 8, the residual exceeds the threshold twice because the faults occur in actuators twice. It can be observed from Figs. 9 and 10 that the faults can be accurately identified by the proposed estimation approach. As shown in Figs. 11 and 12, the attitude and velocity can converge to the vicinity of zero after the first fault is identified. After the second fault occurs, the attitude error and velocity error increase. The FDI mechanism is able to detect and

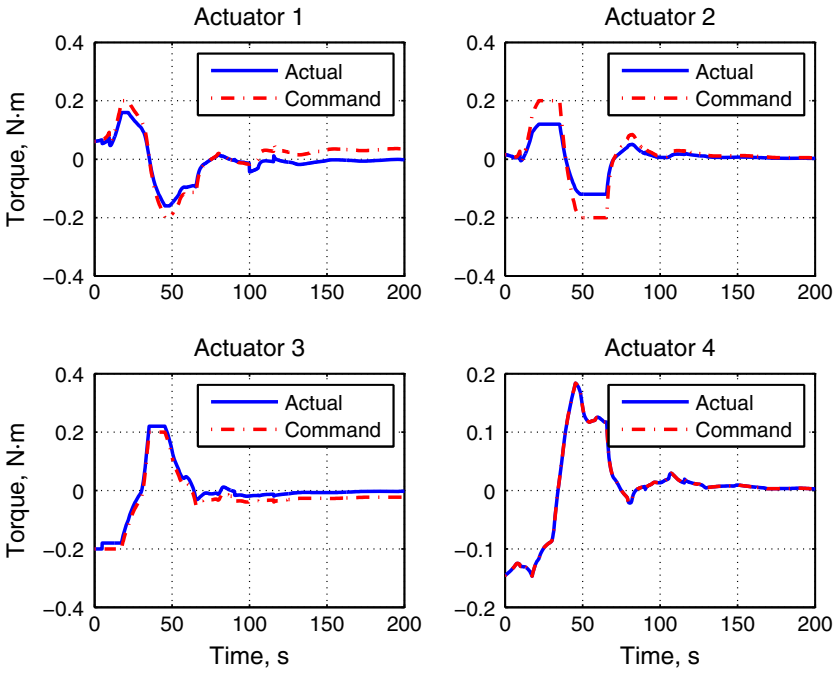

Fig. 13 Command and actual torques (S2).

identify the fault and, in turn, the controller is reconfigured so that satellite attitude and velocity again converge to zero. It can be noted from Fig. 13 that controller switching is carried out during attitude maneuver.

VI. Conclusions

In this Note, active fault-tolerant control for satellite attitude stabilization is investigated. An observer-based fault detection approach is developed that can guarantee that there is no false alarm for the fault in the presence of system uncertainties and external disturbances if there is no noise in the measured signal. A local fault identification approach using past reaction-wheel angular velocity and command input is designed to guarantee asymptotical convergence of the estimated fault to the true value. Based on the proposed fault detection and identification mechanism, an active fault-tolerant control scheme consisting of a reconfigurable controller and control allocation is developed to achieve attitude stabilization. Simulation results have been presented to illustrate the effectiveness of the proposed approaches.

References

[1] Blanke, M., Izadi-Zamanabadi, R., Bosh, S. A., and Lunau, C. P., "Fault-Tolerant Control Systems—A Holistic View," *Control Engineering Practice*, Vol. 5, No. 5, 1997, pp. 693–702. doi:10.1016/S0967-0661(97)00051-8

[2] Zhang, Y. M., and Jiang, J., "Bibliographical Review on Reconfigurable Fault-Tolerant Control Systems," *Annual Reviews in Control*, Vol. 32, No. 2, 2008, pp. 229–252. doi:10.1016/j.arcontrol.2008.03.008

[3] Cai, W. C., Liao, X. H., and Song, Y. D., "Indirect Robust Adaptive Fault-Tolerant Control for Attitude Tracking of Spacecraft," *Journal of Guidance, Control, and Dynamics*, Vol. 31, No. 5, 2008, pp. 1456–1463. doi:10.2514/1.31158

[4] Hu, Q. L., Xiao, B., and Zhang, Y. M., "Fault-Tolerant Attitude Control for Spacecraft Under Loss of Actuator Effectiveness," *Journal of Guidance, Control, and Dynamics*, Vol. 34, No. 3, 2011, pp. 927–932. doi:10.2514/1.49095

[5] Shen, Q., Wang, D., Zhu, S., Poh, E. K., and Liu, T., "Adaptive Robust Fault-Tolerant Attitude Control of Spacecraft with Finite-Time Convergence," *Proceedings of the 9th Asian Control Conference*, IEEE, Piscataway, NJ, 2013, pp. 1–6. doi:10.1109/ASCC.2013.6606131

[6] Shen, Q., Wang, D., Zhu, S., and Poh, E. K., "Finite-Time Fault-Tolerant Attitude Stabilization for Spacecraft with Actuator Saturation," *IEEE Transactions on Aerospace and Electronic Systems*, Vol. 51, No. 3, 2015, pp. 2390–2405. doi:10.1109/TAES.2015.130725

[7] Jiang, T., and Khorasani, K., "A Fault Detection, Isolation and Reconstruction Strategy for a Satellite's Attitude Control Subsystem with Redundant Reaction Wheels," *IEEE International Conference on Systems, Man and Cybernetics*, IEEE, Piscataway, NJ, 2007, pp. 3146–3152. doi:10.1109/ICSMC.2007.4413851

[8] Chen, W., and Saif, M., "Observer-Based Fault Diagnosis of Satellite Systems Subject to Time-Varying Thruster Faults," *Journal of Dynamic Systems, Measurement, and Control*, Vol. 129, No. 3, 2007, pp. 352–356. doi:10.1115/1.2719773

[9] Tudoroiu, N., and Khorasani, K., "Satellite Fault Diagnosis Using a Bank of Interacting Kalman Filters," *IEEE Transactions on Aerospace and Electronic Systems*, Vol. 43, No. 4, 2007, pp. 1334–1350. doi:10.1109/TAES.2007.4441743

[10] Boskovic, J. D., Bergstrom, S. E., Mehra, R. K., Urnes, J. M., Hood, M., and Lin, Y., "Fast On-Line Actuator Reconfiguration Enabling (Flare) System," *AIAA Guidance, Navigation, and Control Conference*, AIAA Paper 2005-6339, 2005. doi:10.2514/6.2005-6339

[11] Boskovic, J. D., Redding, J., and Mehra, R. K., "Integrated Health Monitoring and Adaptive Reconfigurable Control," *AIAA Guidance, Navigation, and Control Conference and Exhibit*, AIAA Paper 2007-6423, 2007. doi:10.2514/6.2007-6423

[12] Boskovic, J. D., Li, S.-M., and Mehra, R. K., "Intelligent Control of Spacecraft in the Presence of Actuator Failures," *Proceedings of the 38th IEEE Conference on Decision Control*, Vol. 5, IEEE, Piscataway, NJ, 1999, pp. 4472–4477. doi:10.1109/CDC.1999.833245

[13] Jiang, T., Khorasani, K., and Tafazoli, S., "Parameter Estimation-Based Fault Detection, Isolation and Recovery for Nonlinear Satellite Models," *IEEE Transactions on Control Systems Technology*, Vol. 16, No. 4, 2008, pp. 799–808. doi:10.1109/TCST.2007.906317

[14] Xiao, B., Hu, Q., and Friswell, M. I., "Active Fault-Tolerant Attitude Control for Flexible Spacecraft with Loss of Actuator Effectiveness," *International Journal of Adaptive Control and Signal Processing*, Vol. 27, No. 11, 2013, pp. 925–943. doi:10.1002/acs.v27.11

[15] Xiao, B., Hu, Q., Singhose, W., and Huo, X., "Reaction Wheel Fault Compensation and Disturbance Rejection for Spacecraft Attitude Tracking," *Journal of Guidance, Control, and Dynamics*, Vol. 36, No. 6, 2013, pp. 1565–1575. doi:10.2514/1.59839

[16] Xiao, B., Hu, Q. L., Wang, D., and Poh, E. K., "Attitude Tracking Control of Rigid Spacecraft with Actuator Misalignment and Fault," *IEEE Transactions on Control Systems Technology*, Vol. 21, No. 6, 2013, pp. 2360–2366. doi:10.1109/TCST.2012.2237403

[17] Xiao, B., Hu, Q., and Wang, D., "Spacecraft Attitude Fault Tolerant Control with Terminal Sliding Mode Observer," *Journal of Aerospace Engineering*, Vol. 28, No. 1, 2013, pp. 1–15. doi:10.1061/(ASCE)AS.1943-5525.0000331

[18] Zou, A. M., Kumar, K. D., Hou, Z. G., and Liu, X., "Finite-Time Attitude Tracking Control for Spacecraft Using Terminal Sliding Mode and Chebyshev Neural Network," *IEEE Transactions on Systems, Man, and Cybernetics, Part B: Cybernetics*, Vol. 41, No. 4, 2011, pp. 950–963. doi:10.1109/TSMCB.2010.2101592

[19] Costic, B. T., Dawson, D. M., Queiroz, M. S., and Kapila, V., "Quaternion-Based Adaptive Attitude Tracking Controller Without Velocity Measurements," *Journal of Guidance, Control, and Dynamics*, Vol. 24, No. 6, 2001, pp. 1214–1222. doi:10.2514/2.4837

[20] Zhao, D. Y., Li, S. Y., and Zhu, Q. M., "A New TSMC Prototype Robust Nonlinear Task Space Control of a 6 DOF Parallel Robotic Manipulator," *International Journal of Control, Automation and Systems*, Vol. 8, No. 6, 2010, pp. 1189–1197. doi:10.1007/s12555-010-0604-y

[21] Liang, Y. W., Xu, S. D., and Tsai, C. L., "Study of VSC Reliable Designs with Application to Spacecraft Attitude Stabilization," *IEEE Transactions on Control Systems Technology*, Vol. 15, No. 2, 2007, pp. 332–338. doi:10.1109/TCST.2006.883186

[22] Shen, Q., Wang, D., Zhu, S., and Poh, E. K., "Integral-Type Sliding Mode Fault-Tolerant Control for Attitude Stabilization of Spacecraft," *IEEE Transactions on Control Systems Technology*, Vol. 23, No. 3, 2015, pp. 1131–1138. doi:10.1109/TCST.2014.2354260